Electronic Supplementary Material (ESI) for Journal of Materials Chemistry A.

Electronic Supplementary Information

Structural and Electronic Modulation of Conductive MOFs for Efficient Oxygen Evolution Reaction Electrocatalysis

Jiawen Li, Peng Liu, Jianxin Mao, Jianyue Yan, and Wenbo Song*

College of Chemistry, Jilin University, Changchun 130012, P.R. China.

**E-mail: wbsong@jlu.edu.cn*

Contents:

1. Experimental Section

TOF calculation: The TOF values were estimated based on our previous report, resulting in the following formula:[1,2,3]

$$\mathrm{TOF} = \frac{number\ of\ total\ oxygen\ turnovers\ /\ cm^2}{number\ of\ active\ sites\ /\ cm^2}$$

The number of total oxygen turnovers was calculated from the current density by the following equation:

$$\text{Number of } O_2 = \left(J\frac{mA}{cm^2}\right)\left(\frac{1\ C\ s^{-1}}{1000\ mA}\right)\left(\frac{1\ mol\ e^-}{96485.3\ C}\right)\left(\frac{1\ mol\ O_2}{4\ mol\ e^-}\right)\left(\frac{6.022*10^{23}\ O_2\ molecules}{1\ mol\ O_2}\right) = 1.56*10^{15}\ \frac{O_2/s}{cm^2}\ per\ \frac{mA}{cm^2}$$

The number of active sites was regarded as the number of surface sites (Ni-O_4 and Fe-O_4 are regarded as active sites), and calculated by the following formula:

$$\text{Nuber of active sites} = \left(\frac{number\ of\ metal\ sites\ /\ unit\ cell}{Volume\ /\ unit\ cell}\right)^{\frac{2}{3}}$$

Finally, the plot of current density can be converted into a TOF plot according to the following formula:

$$\mathrm{TOF} = \frac{\left(1.56*10^{15}\ \frac{\frac{O_2}{s}}{cm^2}\ per\ \frac{mA}{cm^2}\right)*|J|}{Number\ of\ active\ sites *\ A_{ECSA}}$$

The A_{ECSA} is the electrochemical active surface area, which can be calculated from the following formula, where specific capacitance is C_{dl}, and 40 μF cm^{-2} is a constant to convert capacitance to A_{ECSA}:

$$A_{ECSA} = \frac{specific\ capacitance}{40\ \mu F\ cm^{-2}\ per\ cm^2_{ECSA}}$$

D-band center Analysis: The d-band center (ε_d) was calculated according to following equation:[4]

$$\varepsilon_d = \frac{\int_{-\infty}^{0} N(\varepsilon)\ \varepsilon\ d\varepsilon}{\int_{-\infty}^{0} N(\varepsilon)\ d\varepsilon}$$

Where $N(\varepsilon)$ is the d-band DOS, ε is the energy.

2. PXRD Patterns

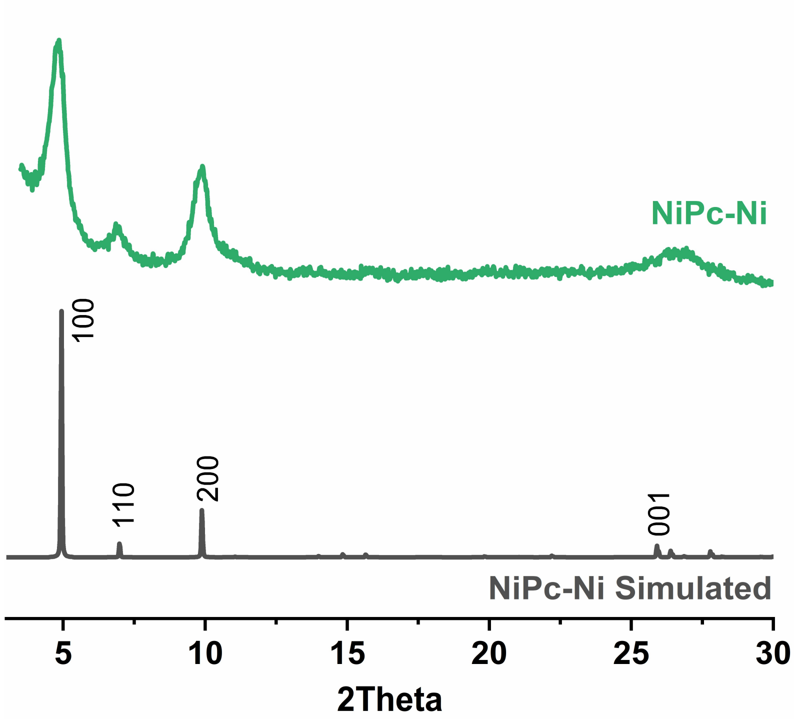

Figure S1. Experimental (green) and simulated (grey) PXRD pattern of NiPc-Ni MOF.

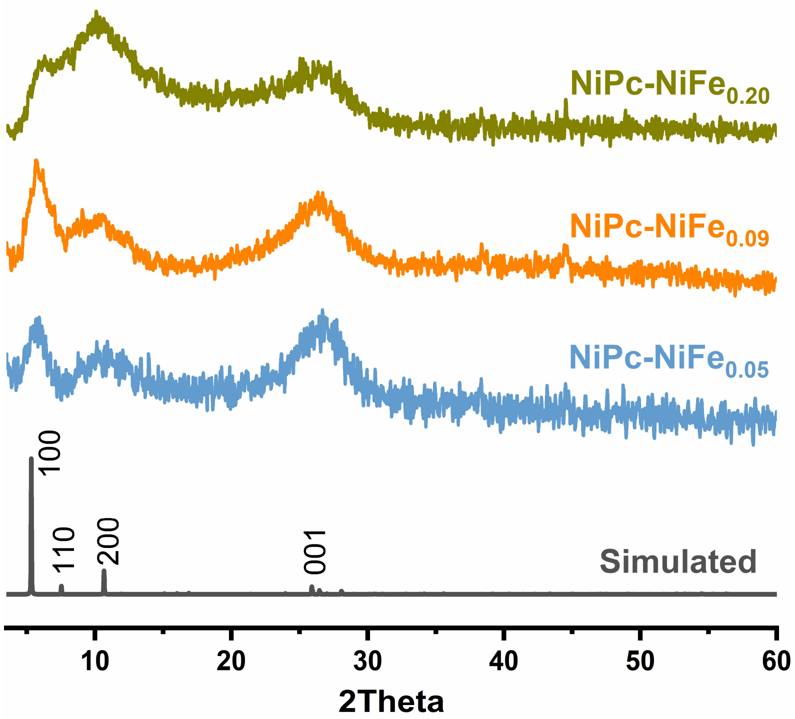

Figure S2. Experimental PXRD patterns of NiPc-$NiFe_{0.05}$, NiPc-$NiFe_{0.09}$, NiPc-$NiFe_{0.20}$, and simulated pattern of NiPc-$NiFe_{0.50}$.

3. SEM and TEM Images

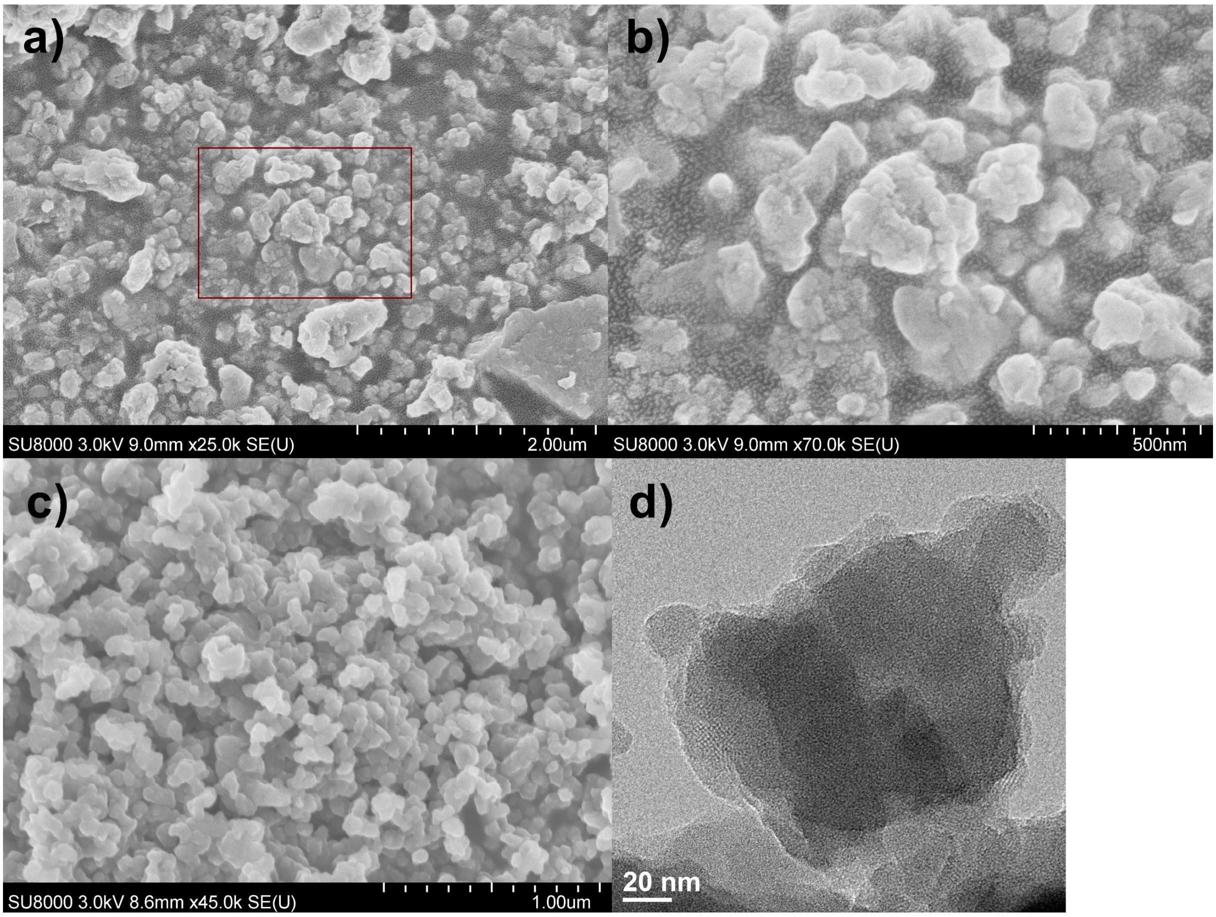

Figure S3. SEM images (a, b) of **NiPc-Fe**, SEM (c) and TEM (d) image of **NiPc-Ni**.

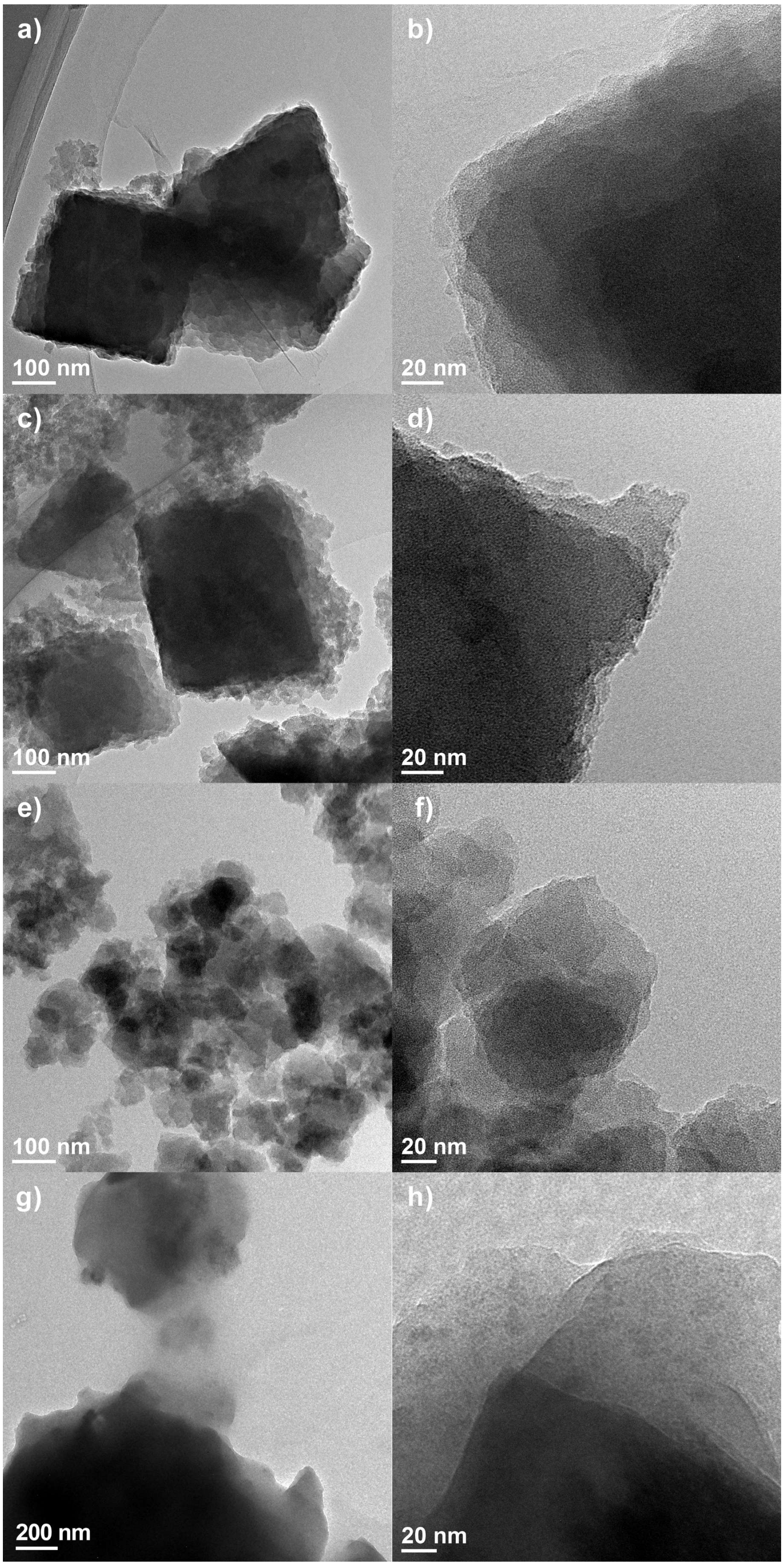

Figure S4. TEM images of **NiPc-NiFe0.05** (a, b), **NiPc-NiFe0.09** (c, d), **NiPc-NiFe0.20** (e, f), **NiPc-Fe** (g, h).

4. XPS Spectra

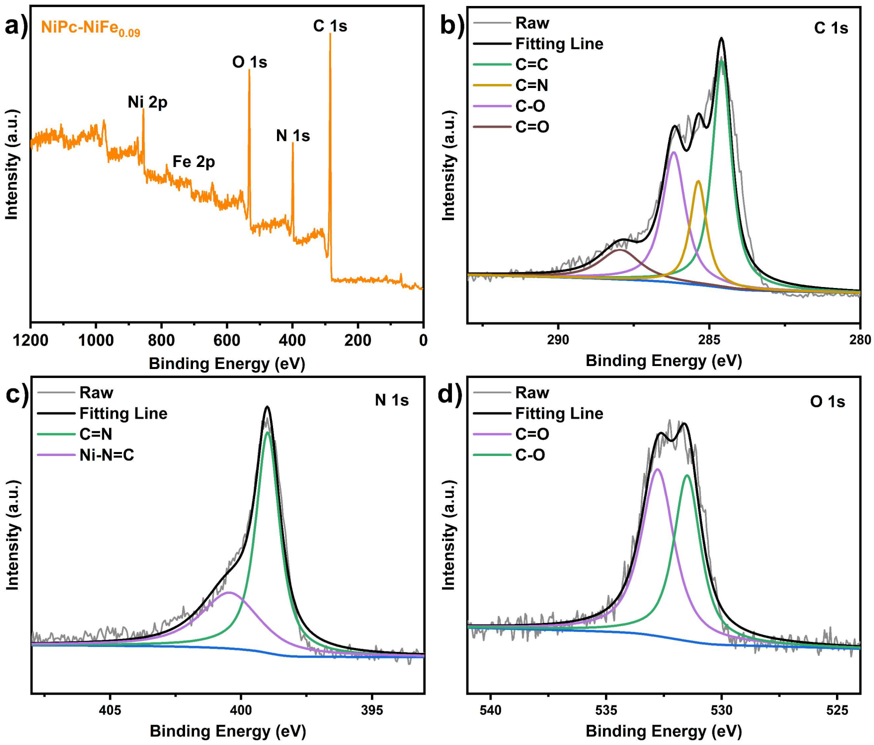

Figure S5. XPS spectra of **NiPc-NiFe0.09**: a) survey, b) C 1s, c) N 1s, d) O 1s. There is an integral ratio of 55:45 for C=O : C-O.

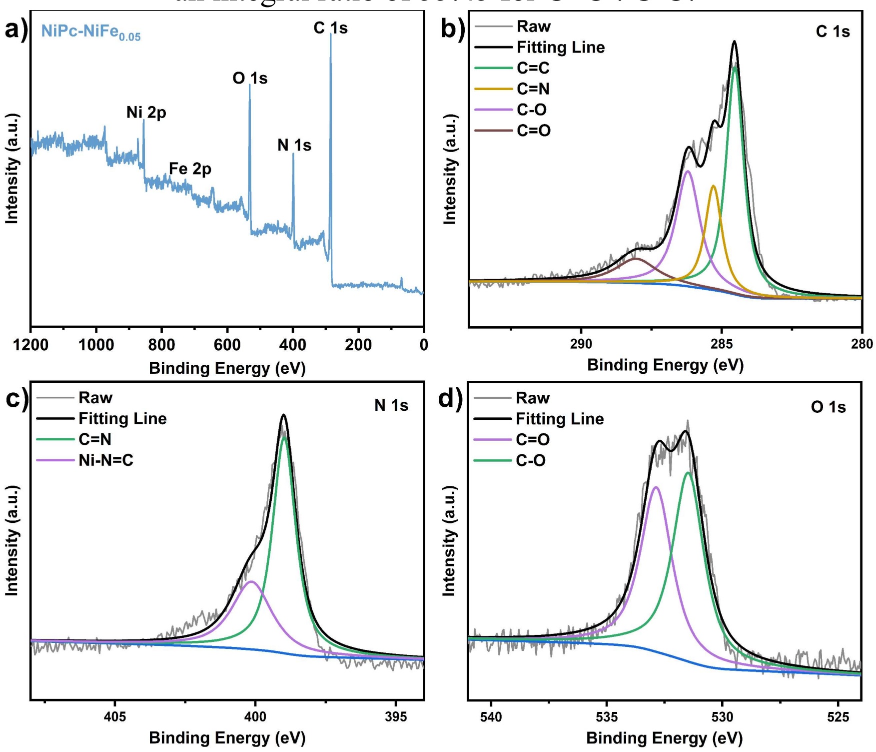

Figure S6. XPS spectra of **NiPc-NiFe0.05**: a) survey, b) C 1s, c) N 1s, d) O 1s. There is an integral ratio of 47:53 for C=O : C-O.

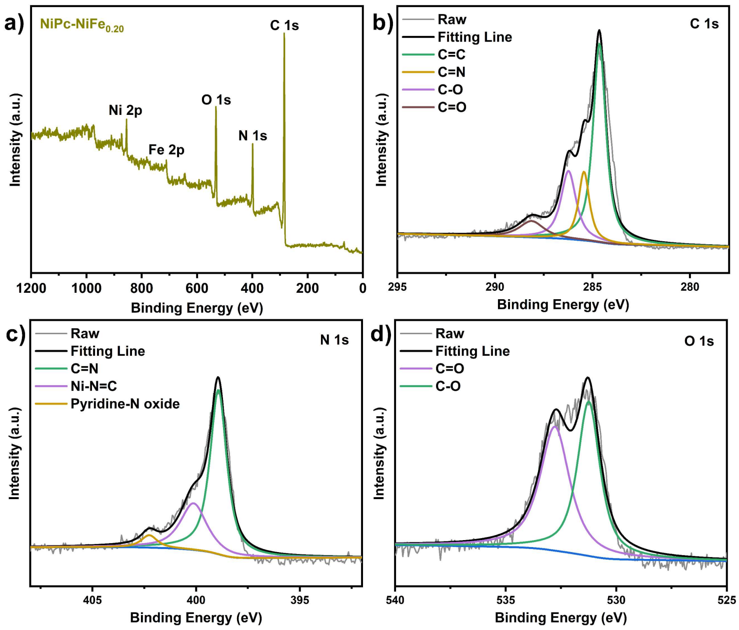

Figure S7. XPS spectra of **NiPc-NiFe0.20**: a) survey, b) C 1s, c) N 1s, d) O 1s. There is an integral ratio of 51:49 for C=O : C-O.

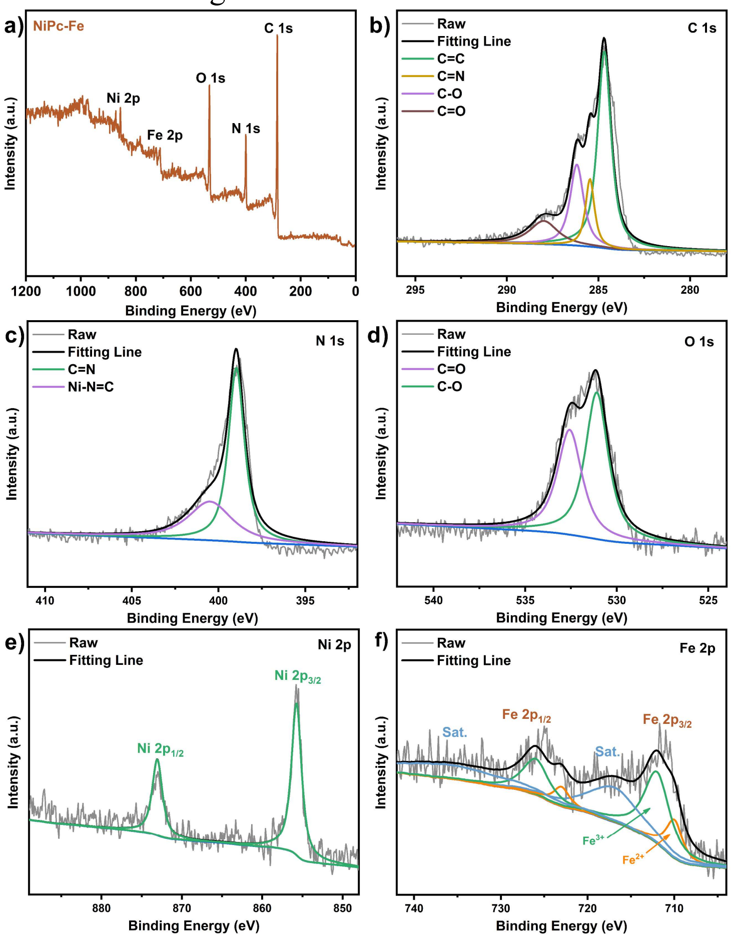

Figure S8. XPS spectra of **NiPc-Fe**: a) survey, b) C 1s, c) N 1s, d) O 1s, e) Ni 2p, f) Fe 2p. There is an integral ratio of 56:44 for C=O : C-O.

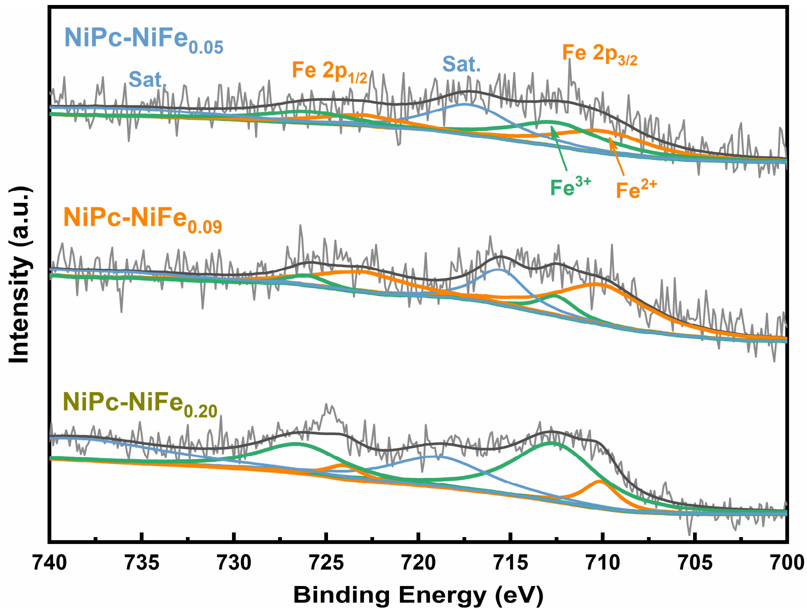

Figure S9. High-resolution Fe 2p XPS spectra of $NiPc-NiFe_{0.05}$, $NiPc-NiFe_{0.09}$, and $NiPc-NiFe_{0.20}$.

5. Linear Sweep Voltammetry

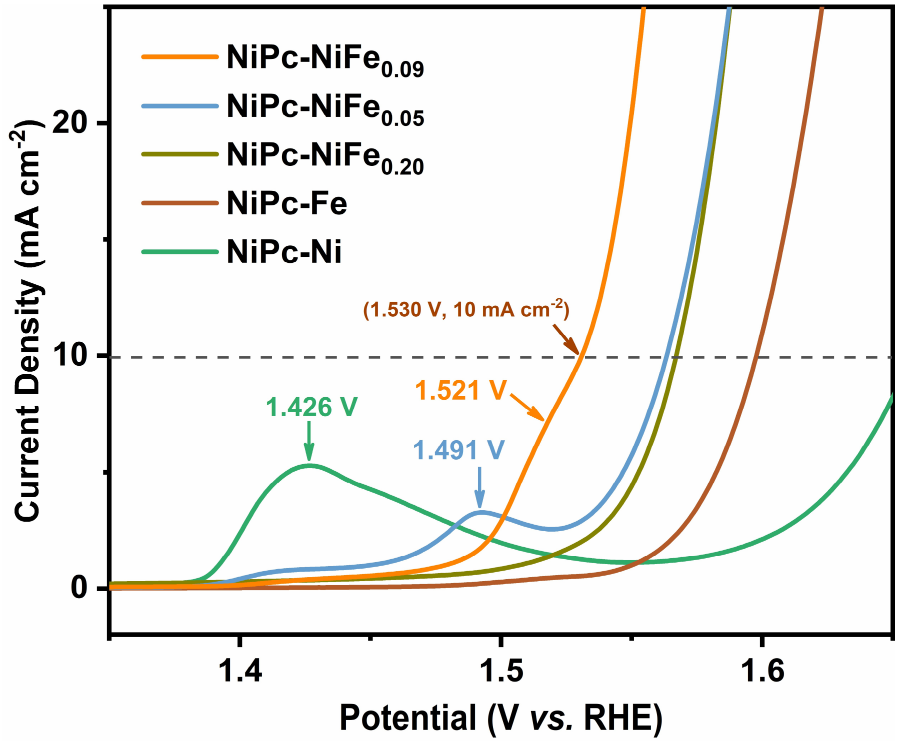

Figure S10. Enlarged LSV plots for OER.

6. ECSA Measurements

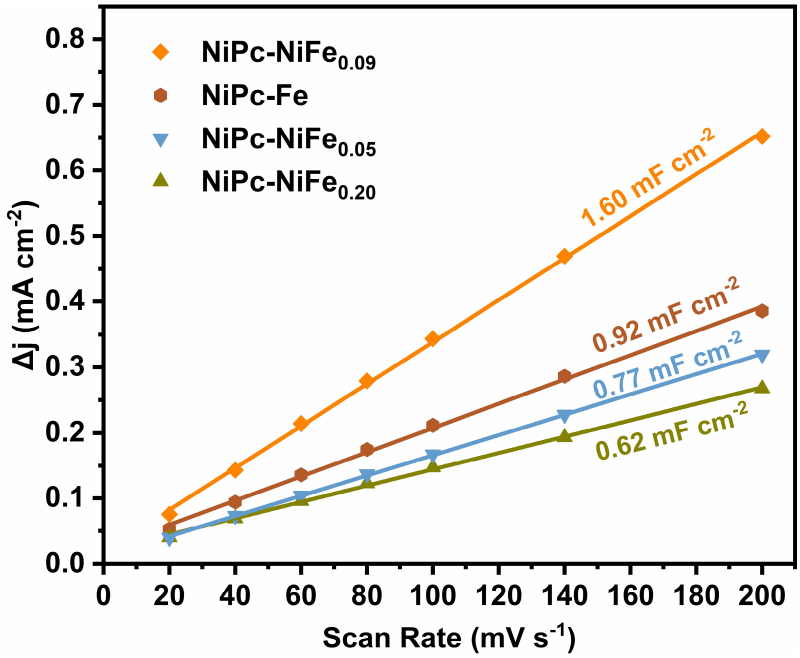

Figure S11. Scan rate dependent-current densities at 0.92 V vs. RHE

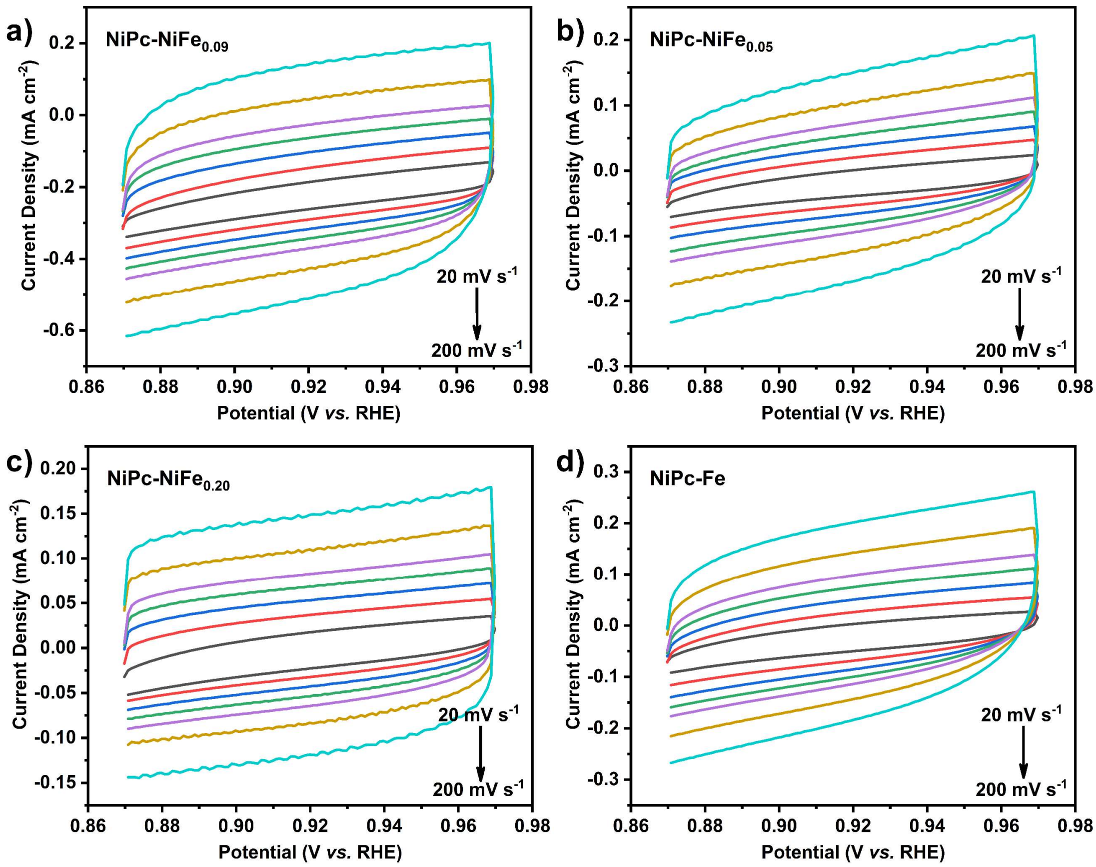

Figure S12. CVs in non-faradaic region of four MOFs.

7. Stability Test

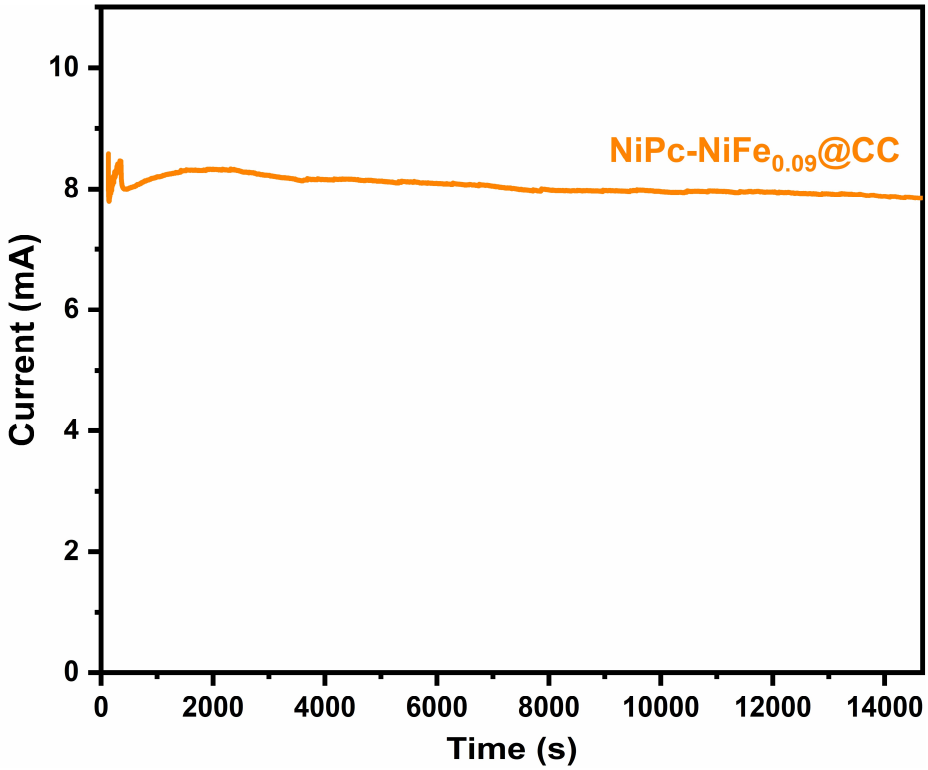

Figure S13. Chronopotentiometry test of NiPc-NiFe$_{0.09}$@CC (Carbon Cloth).

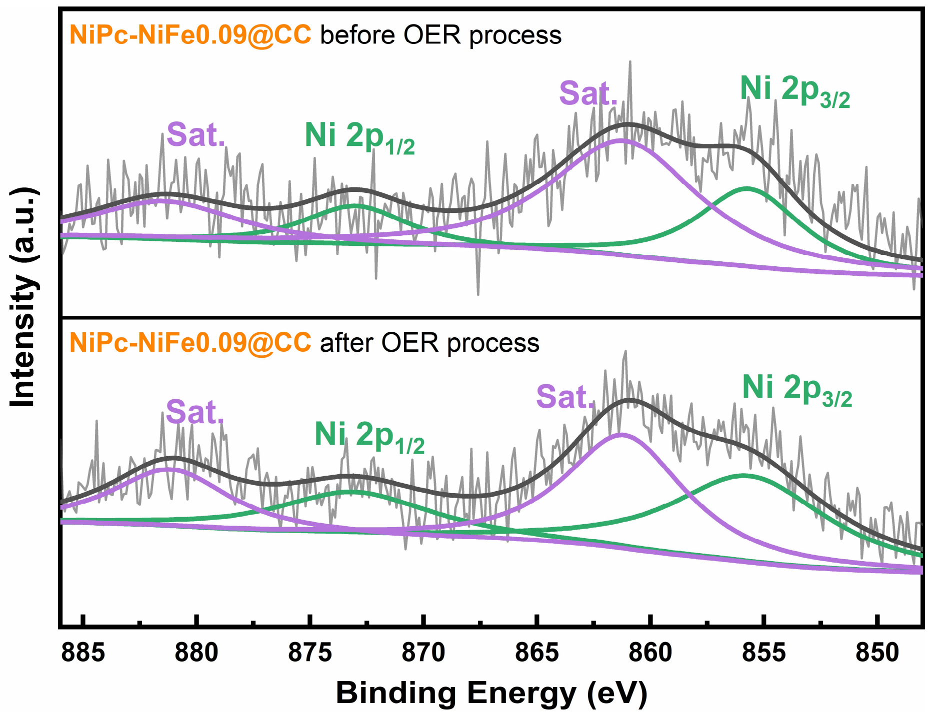

Figure S14. High-resolution Ni 2p XPS spectra before and after Chronopotentiometry test of NiPc-NiFe$_{0.09}$@CC.

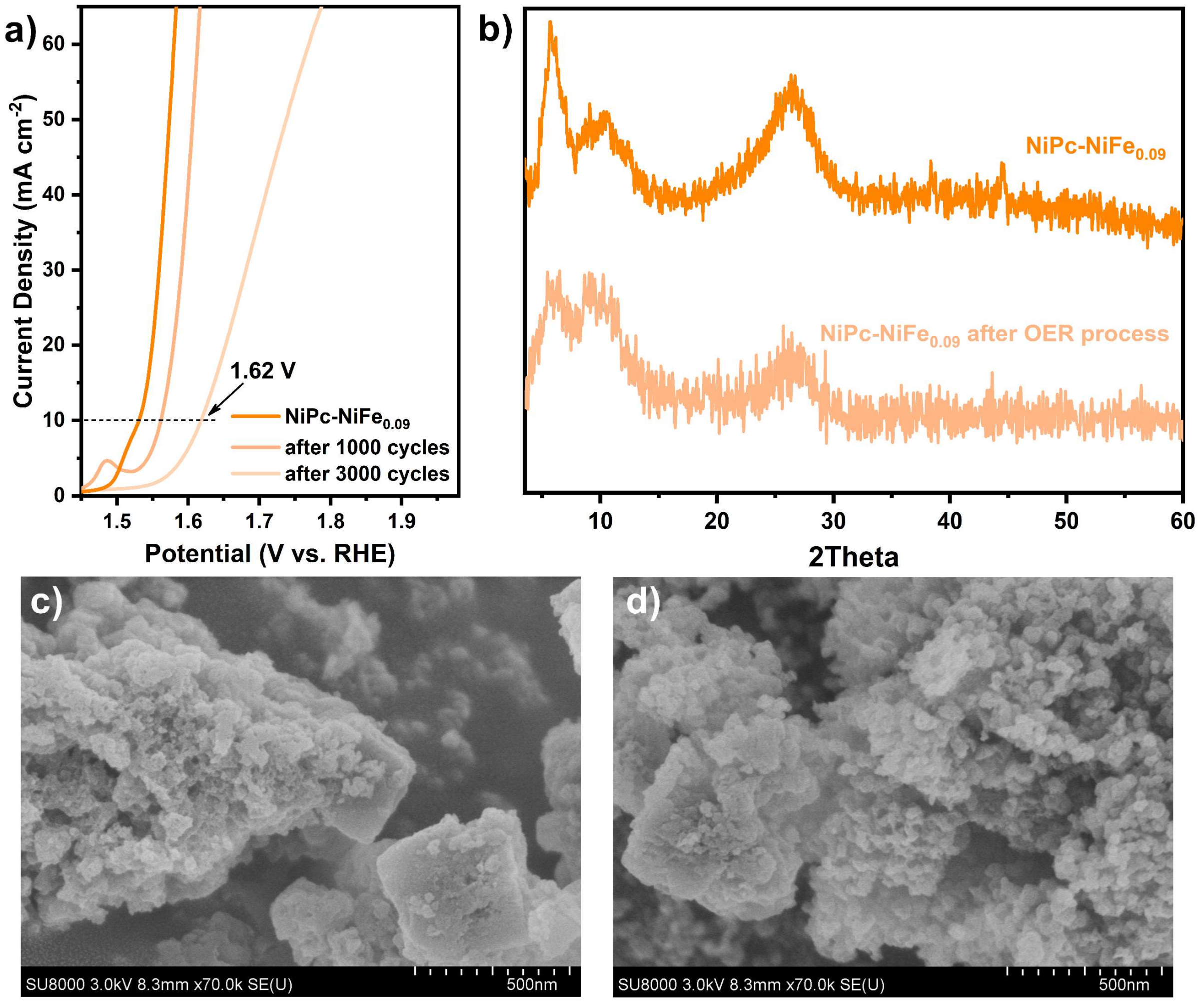

Figure S15. (a) LSV curves of NiPc-NiFe$_{0.09}$ after 3000 CV cycles, (b) PXRD patterns of NiPc-NiFe$_{0.09}$ before and after OER process, (c, d) SEM images of NiPc-NiFe$_{0.09}$ after OER process (3000 CV cycles).

8. Comparison with Commercial Catalyst

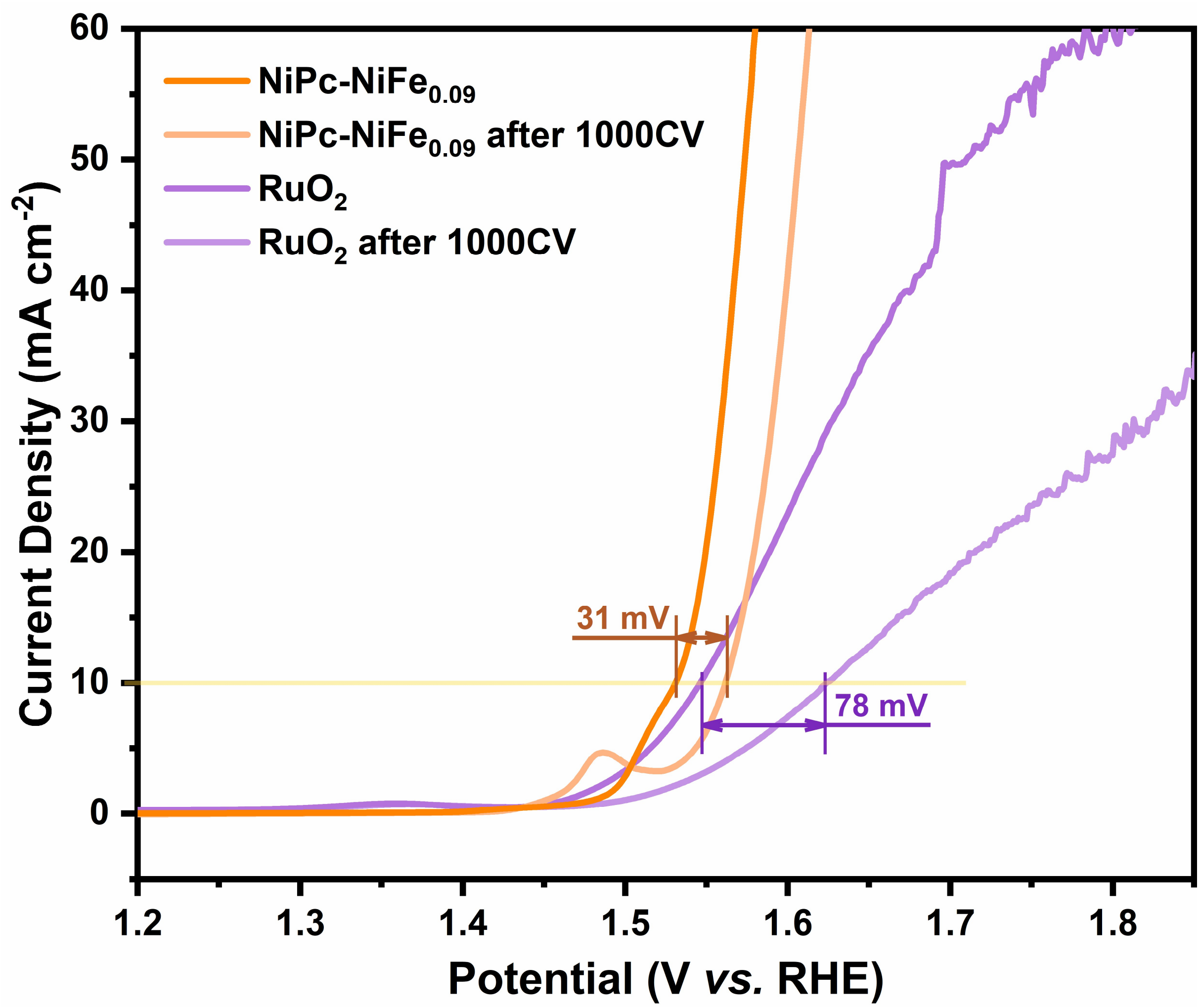

Figure S16. LSV curves of NiPc-NiFe$_{0.09}$ and commercial RuO_2 catalyst before and after 1000 CV cycles, the values in the figure are the shift of η @10 mA cm^{-2} after 1000 CV cycles. Besides, the η of RuO_2 is 317 mV @10 mA cm^{-2}, which is larger than that of NiPc-NiFe$_{0.09}$, indicating the superior OER electrocatalytic performance of NiPc-NiFe$_{0.09}$.

9. Theoretical Calculation Model

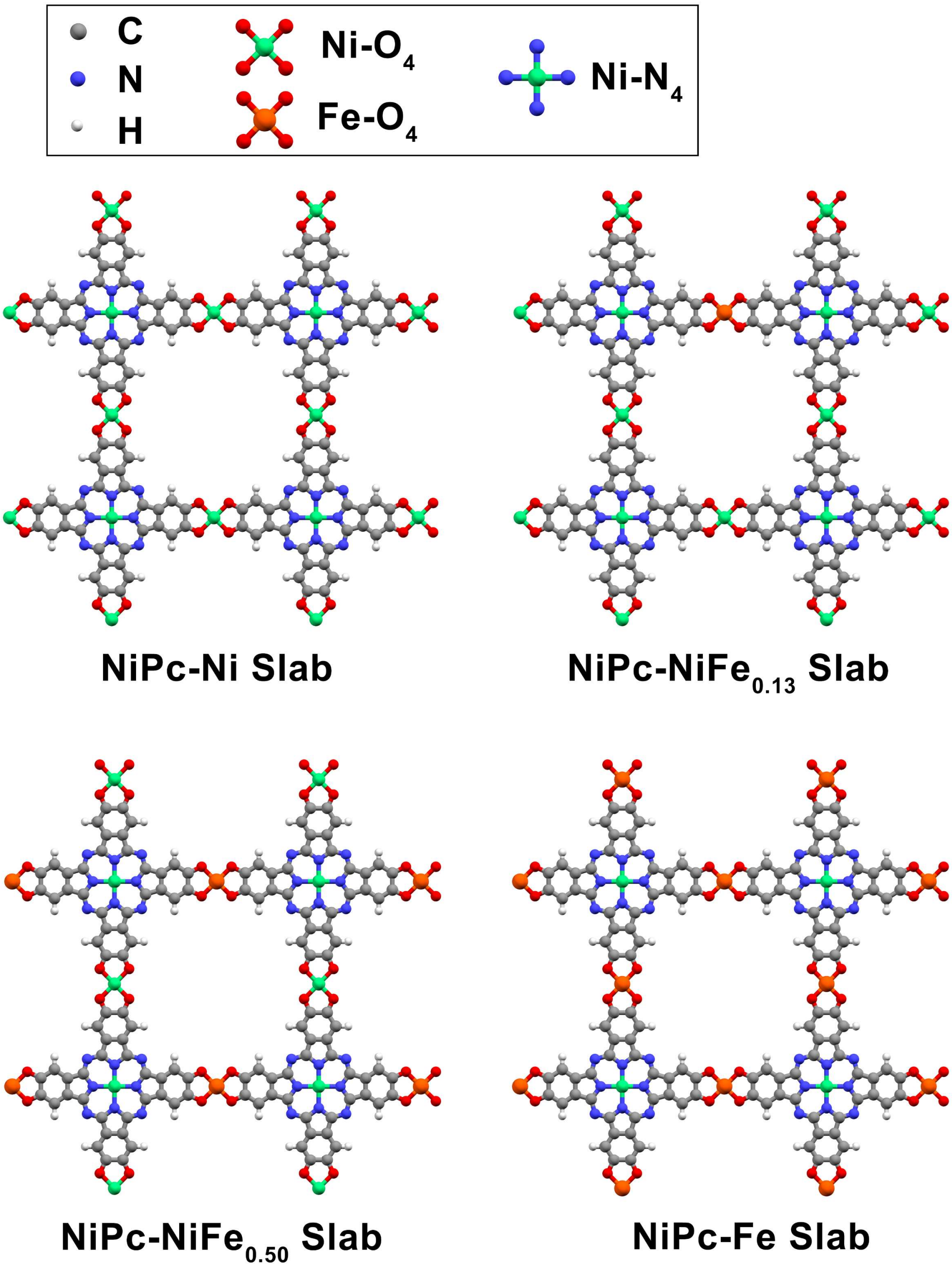

Figure S17. Constructed MOF Slabs for calculation.

10. Comparison Table

Table S1. Comparisons of the OER activity of MOF-based catalysts.

Catalyst	Electrolyte	η @ j=10 mA cm^{-2} (mV)	η @ j=100 mA cm^{-2} (mV)	Tafel slope (mV dec^{-1})	TOF (s^{-1})	Substrate	Ref.
NiPc-NiFe$_{0.09}$	**1.0 M KOH**	**300**	**384**	**55**	**1.943** @η=300 mV **11.943** @η=350 mV	**GC**	**This work**
MAF-X27-OH	1.0 M KOH	387	-	66	0.0014 @η=300 mV 0.038 @η=400 mV	GC	*J. Am. Chem. Soc.*, 2016, **138**, 8336.
Ni-HAB	1.0 M KOH	320	-	51	0.016 @η=300 mV	CFP	*Small*, 2020, **16**, 1907043.
NiCo-UMOFNs	1.0 M KOH	250	-	42	0.86 @η=300 mV	GC	*Nat. Energy*, 2016, **1**, 16184.
Pb-TCPP	1.0 M KOH	470	-	106.2	0.00051 @η=1.2 V	GC	*Dalton Trans.*, 2016, **45**, 61-65.
CUMSs-ZIF-67	1.0 M KOH	410	-	185.1	0.462 @η=300 mV	GC	*Nano Energy*, 2017, **41**, 417-425.
UTSA-16	1.0 M KOH	408	710*	77	-	GC	*ACS Appl. Mater. Interfaces*, 2017, **9**, 7193-7201.
CoNi-Cu(BDC)	1.0 M KOH	327	420*	75.7	-	GC	*New J. Chem.*, 2020, **44**, 2459-2464.
$Ni_{5.7}Ru_{0.3}(HHTP)_3$	0.1 M KOH	390	-	61	-	GC	*Chem. Commun.*, 2020, **56**, 13615-13618.
$[Co_3(HHTP)_2]_n$	0.1 M KOH	490	-	83	-	FTO	*Chem. Commun.*, 2018, **54**, 13579-13582
NNU-23	0.1 M KOH	365	-	81.8	0.03 @η=400mV	CC	*Angew. Chem. Int. Ed.*, 2018, **57**, 9660-9664.

*These values are estimated by LSV plots in the literatures.

11. Equivalent Circuit Parameters for EIS Analysis

Table S2. Fitting Results of these conductive MOFs.

	R_s (Ω cm^2)	*CPE* (mF cm^{-2})	R_p (Ω cm^2)	C_{dl} (mF cm^{-2})	R_{ct} (Ω cm^2)	Z_o (S s$^{0.5}$ cm^{-2})
NiPc-NiFe$_{0.09}$	0.8756	0.3521	0.05715	86.92	0.3315	0.1189
NiPc-NiFe$_{0.05}$	0.7179	1.726	0.139	26.62	1.557	0.1055
NiPc-NiFe$_{0.20}$	0.949	0.1827	0.1603	1.594	2.319	0.02773
NiPc-Fe	0.7634	1.225	3.953	1.078	12.26	0.1232
NiPc-Ni	0.7638	427.2	0.3281	40.17	19.25	0.3553

In the applied module, R_s represents solution resistance, which a combination of contact resistance in the overall circuit and electrolyte. *CPE* represents the constant phase elements. R_p and R_{ct} are on behalf of the resistance of surface porosity and charge-transfer resistance, respectively. C_{dl} represents the double-layer capacitance, which is formed by the adsorption of ions in the solution onto the surface of the electrode. Z_o is limited Warburg impedance, which is originated from finite diffusion layer (such as a thin cell or a coated sample).

The similar value of R_s indicates the conditions of our electrochemical tests are constant. The small value of R_p of NiPc-NiFe$_{0.09}$ demonstrates that this catalyst is highly porous.[5] The value of C_{dl} of NiPc-NiFe$_{0.09}$ is significantly larger than other MOFs, in accordance with its highest electrocatalytic performance. R_{ct} value reflects the ability of charge transfer between electrolyte and electrode. The smallest value of 0.3315 Ω cm^2 of NiPc-NiFe$_{0.09}$ proves the highest electron transport efficiency.

References:

[1] J. Kibsgaard and T. F. Jaramillo, *Angew. Chem. Int. Ed.*, 2014, **53**, 14433-14437.

[2] Z. Liu, Z. Zhao, Y. Wang, S. Dou, D. Yan, D. Liu, Z. Xia and S. Wang, *Adv. Mater.*, 2017, **29**, 1606207.

[3] Z. Chen, Y. Song, J. Cai, X. Zheng, D. Han, Y. Wu, Y. Zang, S. Niu, Y. Liu, J. Zhu, X. Liu, and G. Wang, *Angew. Chem. Int. Ed.*, 2018, **57**, 5076.

[4] H. Wang, J. Wang, Y. Pi, Q. Shao, Y. Tan, and X. Huang, *Angew. Chem. Int. Ed.*, 2019, **58**, 2316.

[5] Y. Huang, J. Ge, J. Hu, J. Zhang, J. Hao, and Y. Wei, *Adv. Energy Mater.*, 2018, **8**, 1701601.